Article

Journal of
Biomedical Nanotechnology
Vol. 19, 1–11, 2023
www.aspbs.com/jbn

Multifunctional Biocompatible *Rhinacanthus nasutus* Based TiO_2-Doped CeO Nanoparticles Synthesis and their Biomedical Evaluations; *In-Vitro*/*In-Vivo* Approach

S. Rajaduraipandian[1], E. Amutha[2], G. Sabeena[2], M. Ponani Kaja Mideen[3], A. Mercy[4], S. Gandhimathi[1], G. Annadurai[2,*], R. Mariselvam[5], Tahani Awad Alahmadi[6], and Sulaiman Ali Alharbi[7]

[1] *Sri Paramakalyani College, Manonmaniam Sundaranar University, Alwarkurichi 627412, India*
[2] *Sri Paramakalyani Centre of Excellence in Environmental Sciences, Manonmaniam Sundaranar University, Alwarkurichi 627412, India*
[3] *School of Chemistry and Chemical Engineering, Central South University, Changsha, China*
[4] *Department of Science and Humanities, J.P. College of Engineering, Ayikudi, Tenkasi 627852 Tamil Nadu, India*
[5] *Saraswathi Institute of Lifescience, Alangulam Main Road, Terkkumadathur, Tenkasi 627423 Tamil Nadu, India*
[6] *Department of Pediatrics, College of Medicine and King Khalid University Hospital, King Saud University, Medical City, P.O. Box-2925, Riyadh, 11461, Saudi Arabia*
[7] *Department of Botany and Microbiology, College of Science, King Saud University, P.O. Box-2455, Riyadh, 11451, Saudi Arabia*

The work intended to evaluate the potential wound healing properties of TiO_2 doped CeO nanoparticles with the assistance of *Rhinacanthus nasutus*. Furthermore, an assessment was conducted on the nanoparticles to determine their antioxidant, cytotoxic, anti-diabetic, and anti-inflammatory inhibitory properties, as well as their toxicity in albino rats. The nanoparticles were synthesized in the green method and subjected to characterization through various methods including UV-visible spectroscopy, SEM for morphological study, FTIR to identify functional groups, XRD, and for elemental analysis EDAX. The morphology of the observed nanoparticles were predominantly spherical, exhibiting an agglomerated structure. The findings indicated that approximately 49% of the nanoparticles exhibited DPPH antioxidant activity, as determined by an IC50 value of 2.8 g/mL. The nanoparticles exhibited cytotoxicity in the brine shrimp lethality assay when administered at a concentration of 50 g/mL. Additionally, they displayed notable inhibitory activity against-amylase, with an IC50 value of 2.981 g/mL. The Ames test yielded negative results, suggesting that the nanoparticles exhibited non-toxic properties. In general, the study substantiated the prospective biological uses of TiO_2-doped CeO nanoparticles.

KEYWORDS: *Nanoparticles, XRD, SEM, Albino Rat.*

INTRODUCTION

Nanoparticles (NPs) have become increasingly important in various fields, including medicine, pharmaceuticals, textiles, and biosensors [1–3]. Metal nanoparticles, in particular, are known for their unique characteristics, such as size, shape, content, and physicochemical properties [2, 4]. In recent times, there has been a significant utilization of metal and metal oxide nanoparticles across various domains, including catalysis, purification of water, batteries, and antimicrobial applications [5]. Cerium oxide nanoparticles (CeO-NPs) have garnered significant interest among researchers owing to their wide range of potential applications [6, 7].

Cerium is classified as a constituent of the lanthanide series and has the capability to exist in two distinct oxidation states, Ce3+ and Ce4+. The rapid change in oxidation state between Ce3+ and Ce4+ has significantly increased biological applications [8]. Cerium oxide nanoparticles can coexist in Ce3+ and Ce4+ on their surface at the nanoscale. Due to oxygen vacancy in the lattice filling the charge deficiency caused by the presence of Ce3+, CeO-NPs naturally possess inherent oxygen defects [9, 10]. These oxygen imperfections serve as catalysts for chemical processes, and with a reduction in particle size, oxygen flaws become more concentrated.

*Author to whom correspondence should be addressed.
Email: gannadurai@msuniv.ac.in
Received: 8 April 2023
Accepted: 3 June 2023

Titanium dioxide (TiO_2) is a naturally occurring metal oxide and an element from the transition metals series. TiO_2 is a white-colored substance found in various products, including paints, rubber, condensers, printing ink, plastics, paper, synthetic fibers, ceramics, electrical components, paints, crayons, food, cosmetics, and more [11]. Cerium-doped TiO_2 nanoparticles are produced using techniques like sol–gel methods, hydrothermal procedures, ball milling, thermal hydrolysis, thermal breakdown, and precipitation [12]. Though, the following limitations still persists like, increased toxicity, high costs, non-eco-friendliness, and chemical usage. To overcome these issues, microorganisms and plants have been employed as precursors.

Using plants as precursors offers several advantages, including easy handling, widespread availability, and a variety of metabolites. The plant extracts consists the following Phytochemicals, like flavonoids, acids, terpenoids, amino proteins, and saponins, carbohydrates, are essential for nanoparticle formation. *Rhinacanthus nasutus*, also known as Snake jasmine, is a herbaceous shrub belonging to the family of Acanthaceae. The origin of this plant can be traced back to Thailand, as well as extensive regions of South and Southeast Asia. *Rhinacanthus nasutus* is known to possess various phytochemical constituents, including Dehydro—lapachone lupeol, stimasterol, vanillate, 2-methylanthraquinone, (+)-praeruptorin, oroxylin syringaldehyde, methyl sitosterol, umbelliferone, glutinol, A, wogonin, α-amyrin, p-hydroxybenzaldehyde, as well as several novel compounds [13]. The ethanol extract derived from the leaves of Rn, which is abundant in rhinacanthin, has demonstrated noteworthy efficacy against Helicobacter pylori, a Gram-negative bacterium that is recognized for its role in the development of ulcers and cancer. The minimum inhibitory concentration (MIC50) required for this extract to inhibit the growth of *H. pylori* was determined to be 0.5 mg/mL [13, 14].

The current research used the leaf extract of *Rhinacanthus nasutus* for the purpose of synthesizing TiO_2 doped CeO nanoparticles through a green synthesis approach. The selection of the extract was based on its potential as an antioxidant, its ability to inhibit cytotoxicity, its anti-diabetic properties, its anti-inflammatory effects, and its potential for wound healing research. The synthesized nanoparticles of TiO_2 doped with CeO were subjected to characterization using various analytical techniques, including a *SEM with EDAX, FT-IR, XRD, and UV*-Spectroscopy.

MATERIALS AND METHOD

Plant Material Collection and Extraction

The medicinal plant *Rhinacanthus nasutus* were collected from Surraikkaipatty, Virudhunagar district, Tamil Nadu in the Latitude and longitude range of 9.587209, and 77.964702. *Rhinacanthus nasutus* leaf was washed repeatedly with water and shade dried for a week. 10 g of dried *Rhinacanthus nasutus* leaves were mixed with 100 mL of $D.H_2O$. The mixture was then steamed for approximately 10 minutes at 90 °C. By using filter paper (Whatman No. 1) the leaf extract was filtered and the resulting filtrate was subsequently stored at a temperature of −4 °C for future utilization.

Preparation of Cerium Oxide Nanoparticles

In brief, the preparation process involved the gradual addition of 20 mL of *Rhinacanthus nasutus* extract to a mixture of 80 mL of 5 mM cerium nitrate solution and 80 mL of deionised water. The pH of the solution was modified to a value of 7 by employing a 1 N sodium hydroxide solution. The resultant mixture was agitated using a magnetic stirrer for a duration of 30 minutes. Following that, the combination underwent a conventional air oven drying process (24 hours at 60 °C) resulting in the attainment of a light brown hue. Centrifugation was then performed to separate the particles from the solution. Finally, the obtained cerium oxide nanoparticles were subjected to calcinations in a muffle furnace at 700 °C for duration of 2 hours.

Preparation of Titanium Doped Cerium Oxide Nanoparticles

To synthesize TiO_2-doped cerium oxide nanoparticles, a solution was prepared by dissolving an equimolar mixture of cerium oxide nanoparticles and titanium dioxide in 100 ml of distilled water. Subsequently, the solution was positioned onto a magnetic stirrer and subjected to agitation at a rotational speed of 400 revolutions per minute (rpm) for a duration of 24 hours. After the completion of the stirring process, the solution underwent filtration using filter paper and was subsequently subjected to oven drying at 60 °C. The resulting TiO_2-doped cerium oxide nanoparticles were further subjected to calcinations in a muffle furnace for duration of 2 hours at a temperature of 700 °C.

Characterization of TiO_2-Doped CeO Nanoparticles

The structural and morphological characteristics of *Rhinacanthus nasutus* plant extract-mediated TiO_2-doped CeO nanoparticles were assessed using SEM with EDAX, FT-IR, XRD, and UV-Spectroscopy techniques.

Anti Diabetic Assay

α Amylase Inhibition Assay

To assess the anti-diabetic activity of TiO_2 doped CeO nanoparticles through an α-amylase inhibition assay was carried out. The nanoparticles were introduced into a solution comprising sodium phosphate buffer (0.02 M) with sodium chloride (6 mM, pH 6.9) at different concentrations (25–100 g/mL) by the researchers. Subsequently, the concoction was subjected to incubation for a duration of 20

minutes at a temperature of 37 °C. Following the incubation period, a 1% (250 μL) starch solution was introduced into the reaction mixture and subjected to an additional incubation period of 15 minutes. The reaction was halted by the introduction of dinitro acid, subsequent to which the mixture was subjected to thermal treatment in a water bath (100 °C) for 10 minutes. This was followed by a cooling process. The measurement of optical density was conducted at a wavelength of 540 nm. In order to establish the control, different concentrations of reaction solutions lacking nanoparticles and insulin (ranging from 25 to 100 g/mL) were employed to create both negative and positive control samples. The determination of α-amylase inhibition percentage was conducted utilizing the subsequent formula.

$$\% \text{ inhibition} = [(\text{A\_t} - \text{A\_p})\text{A\_t}] \times 100$$

Here, A_t = control absorbance, A_p = sample absorbance.

Wound Healing Study

Wound healing activities were observed by using Albino rats, overall 12 albino rats were observed. Wound was created through surgical blades. We separate them on the basis of equal counting on 3 Groups. Group 1–Control, Group 2–TiO_2 doped CeO and group-3 TiO_2 doped CeO nanoparticles. Group 1 was treated with distilled water alone. The mice in Group 2 were subjected to the administration of a suspension containing TiO_2 doped CeO in distilled water, with a dosage of 1 mg, for the purpose of promoting wound healing. This treatment was carried out over a duration of 4 weeks. A suspension of group-3 TiO_2 doped CeO nanoparticles was prepared by dispersing them in distilled water at a consistent dosage and for identical durations. After a treatment period of four weeks, it was observed that all mice in the three experimental groups achieved a state of recovery, with the extent of their cure being contingent upon the specific dosages administered. Ultimately, the wound healing levels of all the albino rats were assessed.

Acute Toxicity Studies Using TiO_2 Doped CeO Nanoparticles

Titanium dioxide (TiO_2) doped cerium oxide (CeO) nanoparticles through experimentation involving a group of six mice is used to carryout acute toxicity study. The mice were allocated into two groups using randomization, with each group consisting of three animals. Group 1 was designated as the control group, whereas Group 2 underwent treatment involving the utilization of titanium dioxide-doped cerium oxide nanoparticles. The nanoparticles suspended in distilled water were orally administered to the mice in Group 2 at a dose of 1.5 mg/kg bwt/day for ten days. Double-distilled water was the only treatment given to the control group mice.

All mice in both groups were fasted overnight and euthanized the following day. Haematological and histological analyses were performed to determine the toxicity at the end of the ten-day treatment period.

Brine Shrimp Lethality Assay

Salt Water Preparation

To initiate the experiment, dissolve a quantity of 2 grams of iodine-free salt in 200 milliliters of water that has been filtered. Subsequently, the process of preparing six ELISA plates involves the addition of 10–12 mL of saline water to each individual well. Then, gently add 10 nauplii to each well using 10 μL, 20 μL, 30 μL, 40 μL, 50 μL, and a control well. Add the appropriate concentration of TiO_2 doped CeOnanoparticles to each well and incubate the plates for 24 hours. After a duration of 24 hours, the ELISA plates should be observed in order to enumerate the viable nauplii and subsequently approximate their quantity utilizing the provided formula.

$$\text{Number of dead nauplii/Number of dead nauplii} + \text{Number of live nauplii} \times 100$$

In Vitro Antioxidant Assay

The capacity of TiO_2 doped CeO nanoparticles to remove free radicals was assessed through the utilization of the DPPH technique. A mixture was prepared by combining a suspension of CeO nanoparticles doped with TiO_2 in water (3 mL) with a solution of DPPH in methanol (250 mL) at a concentration of 0.3 mM (0.5 mg of DPPH dissolved in 12 mL of methanol). The resulting mixture was prepared at various concentrations (5, 10, 25, and 50 g/mL). The control sample was generated by the amalgamation of 3 mL of water with 250 mL of DPPH. The experiment was conducted three times independently to determine the average value. The calculation of the percentage inhibition (% PI) of the DPPH radical, which serves as a measure of the antiradical activity, was performed by assessing the reduction in absorbance caused by the addition of test materials. The determination of the ability to eliminate the DPPH radical was conducted using Eq. (1) as described in this study.

$$\text{DPPH Scavenged } (\%) = (Ac - As/Ac) \times 100 \quad (1)$$

In which the Ac indicates control absorbance and As sample absorbance (at 517 nm, after 30 min). In order to calculate the sample's IC50 value, a linear regression analysis was used.

Anti-Inflammatory Activity

To evaluate the anti-inflammatory effect of TiO_2 doped CeO nanoparticles, the Mizushima and Kobayashi method was adapted. By adding 0.45 mL of a 1% aqueous solution of bovine serum albumin to 0.05 mL of TiO_2 doped

CeO nanoparticles to adjust the pH of the mixture to 6.3 nat various concentrations ranging from 10 μL to 50 μL. Careful micro-pipetting was employed to prevent any bias, and previously collected standard values were used for comparison [15]. The samples were then subjected to heating for 30 minutes in water bath (55 °C), following 20-minute incubation at room temperature. Following the cooling process, the absorbance at a wavelength of 660 nm was quantified utilizing a spectrophotometer. The reference standard employed for comparative analysis was diclofenac sodium, while the control substance utilized was dimethyl sulfoxide (DMSO).

The equation utilized in this study has been used to determine the protein denaturation percentage:

$$\% \text{ inhibition} = (\text{Absorbance of control} - \text{Absorbance of sample} \times 100) / \text{Absorbance of control}$$

Statistical Analysis

To compare various groups, the gathered data were statistically analysed using one-way ANOVA and Duncan's post hoc test. At a *P*-value of 0.005, the difference between the groups was deemed significant. The mean and SEM of the data are displayed. The analyses were conducted utilizing SPSS version 26.0.

RESULTS AND DISCUSSION

Characterization

UV-Spectroscopy is one of the familiar analytic techniques. This is used to analysis the sample which absorbs the intensity of light. In this, it discuss about the UV light absorption in TiO_2 doped CeO nanoparticles with *Rhinacanthus nasutus* leaf extract. The UV-Spectrum of green synthesised TiO_2 doped CeO nanoparticles using *Rhinacanthus nasutus* leaf extract is shown in Figure 1. The TiO_2 doped CeO nanoparticles absorption in UV-measurement in the wavelength range of 250–400 nm. Particularly, the wavelength at 325 nm for CeO [16] and 387 nm for TiO_2. In addition, the absorption spectrum exhibited a prominent peak at a wavelength of 300 nm, indicating the presence of intrinsic band-gap absorption in TiO_2 doped CeO nanoparticles. The observed phenomenon of absorption can be explained by the occurrence of electron transitions from the valence band to the conduction band. The presence of a peak in the absorption spectrum at approximately 300 nm suggests the formation of nanoparticles consisting of CeO doped with TiO_2 [17].

FTIR (Fourier-transform infrared spectroscopy) is a widely employed analytical technique, which is employed to analyse functional groups present in the sample. In Figure 2, the FTIR spectrum of TiO_2 doped CeO nanoparticles using *Rhinacanthus nasutus* leaf extract is shown. FTIR spectra observed at a wave number range of 4000–400 cm^{-1} Here various peaks are recorded at 3450,

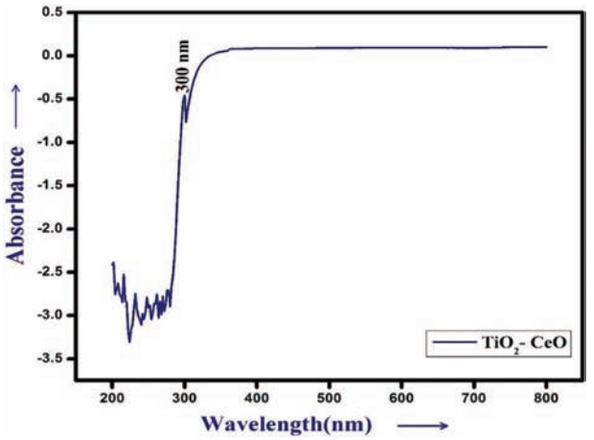

Figure 1. **UV-Spectrum of TiO_2 doped CeO nanoparticle using *R.nasutus* leaf extract.**

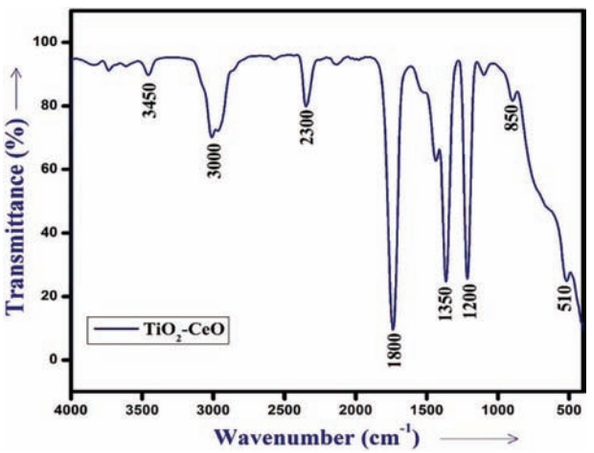

Figure 2. **FTIR-Spectrum of TiO_2 doped CeO nanoparticles using *R.nasutus* leaf extract.**

3000, 2300, 1800, 1350, 1200, 850, 510 cm^{-1}. The first peak at 3450 cm^{-1}, which belongs to the range of 3550–3200 cm^{-1}, it indicates O–H stretching i.e., alcohol. Next peak at 3000 cm^{-1}, it between the range of 3000–2840 cm^{-1} which indicates the –H stretching i.e., alkane [18]. The wave number 2300 cm^{-1} it slightly near at 2349 cm^{-1} thus represents the C═O═C stretching i.e., carbon dioxide. Acid halide (C═O stretching) has wave number range of 1815–1785 cm^{-1} and here is the wave number observed at 1800 cm^{-1}. The intense peak at a wave number 1350 cm^{-1} it represent that S═O stretching sulfo compound. The intense peak observed at 1200 cm^{-1}, it is in the range of 1225–1200 cm^{-1} represents C–O stretching i.e., vinyl ether [18]. The halo compound has a range between 850–550 cm^{1} (C-X stretching) here is the range at 850 & 510 cm^{1}.

Scanning electron microscope (SEM) is the most important microscopic technique due to its ability to image materials and structures with sub-micron level resolution. This

technique enforced to analyses morphology and crystallography. It has important function which is accurate measurement of the surface topography of a material with spatial resolution [19].

This SEM analysis revealed the morphology and aggregate formation of *Rhinacanthus nasutus* leaf extract-derived green TiO_2 doped CeO nanoparticles, as shown in Figure 3. These results confirm the formation of nanoparticles is spherical, cube with less agglomeration and undefined structure [20].

The SEM is equipped with Energy Dispersive X-ray spectroscopy (EDAX) capabilities. The analysis involved the examination of the sample's percentage and composition. Figure 4 depicts the EDAX outcome of greenly synthesized TiO_2 doped CeO nanoparticles made with *Rhinacanthus nasutus* leaf extract. This result shows the various components present in the sample such as Ti, Ce, O. Sharp peaks (strong signal) confirms the sample have Ti, Ce, O [21]. The percentage of main components Ti, Ce and O are present in a sample is given below Table I. Weight percentages of components are Oxygen has 33.7%, Titanium has 37.7% and Cerium has 28.6%.

X-ray diffraction spectroscopy (XRD) technique is the rapidly analyzing crystallographic technique. It used to analysis the crystalline structure. The X-ray diffraction spectra of TiO_2 nanoparticles doped with CeO, synthesized through a green method utilizing *Rhinacanthus nasutus* leaf extract, are presented in Figure 5. In this XRD spectra shows the Bragg's reflection related to 25.10, 28.39, 32.92, 37.58, 47.86, 56.22 and 62.55 that indexed the plane 101, 111, 200, 104, 220, 211 and 204 respectively [15]. The Peaks exhibit a congruence with the JCPDS (Joint Committee on Powder Diffraction Standards). The Debye-Scherrer formula was employed to determine the average crystalline size of TiO_2 doped CeO nanoparticles synthesized through a green method employing *Rhinacanthus nasutus* leaf extract.

$$D = (k\lambda)/(\beta \cos\theta)$$

In the given equation, the variable D represents the particle size, measured in nanometers. The constant k has a value of 0.94. The variable λ denotes the X-ray wavelength, which is equal to 1.5406. The variable θ denotes the angular measure, expressed in radians, that corresponds to the full-width at half maximum (FWHM) of the peak. Lastly, the variable α represents the Bragg angle, measured in degrees. The study determined that the mean diameter of the TiO_2-doped CeO nanoparticles, which were synthesized using a green method involving the utilization of *Rhinacanthus nasutus* leaf extract, was in the range of of 22.23 nm [22].

Applications

Anti-Diabetic Activity

The findings pertaining to the inhibition of α-amylase are visually represented in Figure 6. Irrespective of the specific field of study, this research focuses on the utilization of TiO_2 doped with CeO nanoparticles. The CeO nanoparticles doped with TiO_2 exhibit inhibitory activity against α-amylase, suggesting a potential anti-diabetic effect. Delaying the rate of starch digestion can potentially result in a delay in the absorption of glucose. If the activity of the mammalian α-amylase enzyme in the intestine was inhibited, the breakdown of starch and oligosaccharides into monosaccharides would not occur, leading to their inability to be absorbed. The intervention being proposed would result in a decline in glucose absorption, leading to a subsequent decrease in blood glucose levels after a meal [23]. Hence, the inhibition of α-amylase by TiO_2-doped CeO nanoparticles suggests that these nanoparticles have the potential to mitigate postprandial hyperglycemia and its associated diabetic complications. This finding further substantiates the long-standing utilization of *Rhinacanthus nasutus* for the management of diabetes [24]. Studies have provided evidence that the incorporation of TiO_2 into CeO nanoparticles yields promising results as inhibitors for diabetes mellitus. Based on their perspective, TiO_2 doped

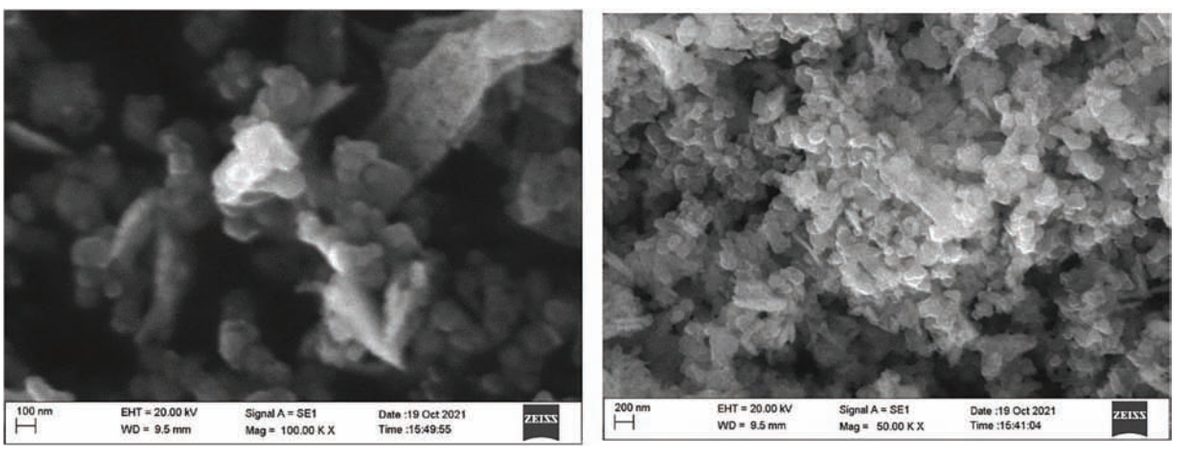

Figure 3. **Scanning electron microscopic image of TiO_2 doped CeO nanoparticles using *R.nasutus* leaf extract.**

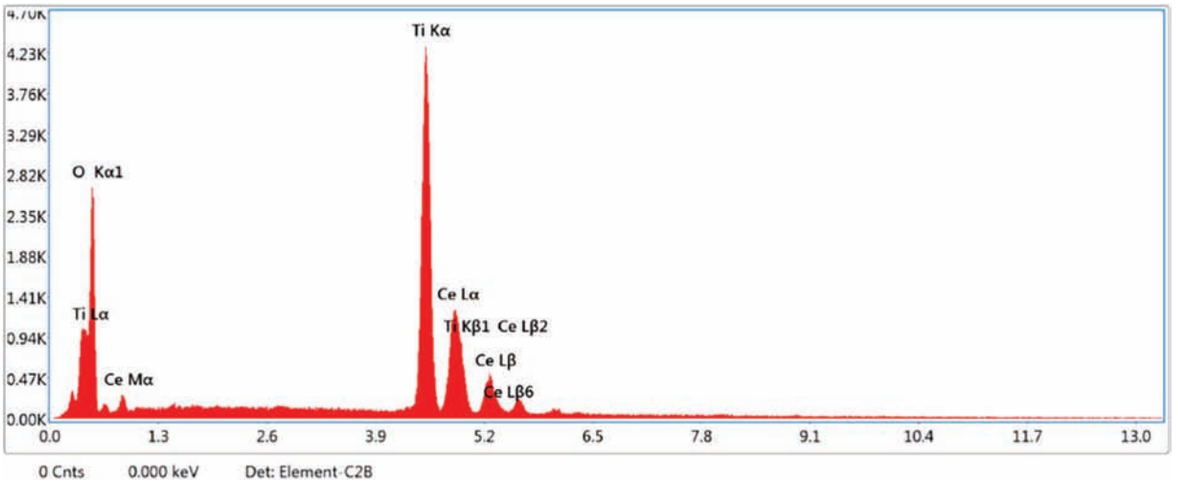

Figure 4. **Energy dispersive X-ray spectroscopy report of TiO_2 doped CeO nanoparticles using *R. nasutus* leaf extract.**

CeO nanoparticles have a good antidiabetic activity. Compared to the control the nanoparticles shows higher anti diabetic activity. At the Initial stage the concentration level of 10 μg/mL only 42% of inhibition in control and 55% of inhibition of TiO_2 doped CeO nanoparticles. At the concentration level of 50 μg/ml control attains 68% and 78% of inhibition in TiO_2 doped CeO nanoparticles. Finally, TiO_2 doped CeO nanoparticles have excellent antidiabetic medicine, It is confirmed by these study.

Wound Healing Study

For the study on wound healing, green synthesis nanoparticles, plant extract, and TiO_2 doped CeO nanoparticles were used (Fig. 7). When compared to control, rats given TiO_2 doped CeO nanoparticles made using green synthesis and plant extract showed initial signs of healing. Additionally, it was found that the rats treated with plant extract alone and green synthesis TiO_2 doped CeO nanoparticles displayed greater healing responses than the control rats four weeks after injury. The percentage of lesions that had healed in the four weeks following treatment for the four groups—control, plant extract, with green synthesis TiO_2 doped CeO nanoparticles—was 54%, 60%, 70%, and 80%, respectively. These findings suggest that the most potent healing action is produced by the plant extract with CeO Nanoparticles doped with TiO_2 [25]. This study aimed to investigate the temporal dynamics of healing wounds across various treatment groups and to explore the activation of apoptosis in the context of healing wounds.

Toxicity Study of Mouse Organs

In this experimental investigation, laboratory mice were administered oral injections of CeO Nanoparticles that were doped with TiO_2. The dosage administered to the mice was 1.5 mg per kilogram of body weight per day, and

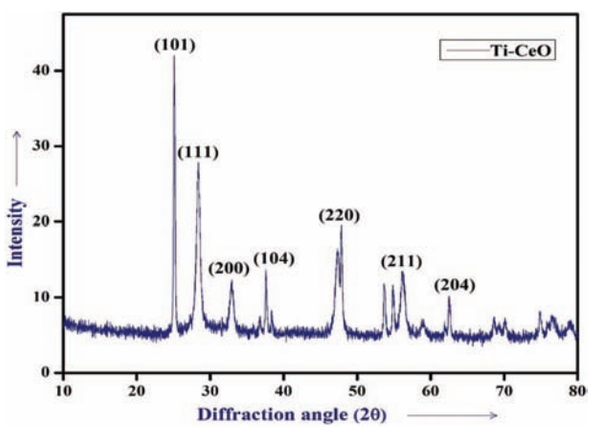

Figure 5. **X-ray diffraction spectra for TiO_2 doped CeO nanoparticles using *R. nasutus* leaf extract.**

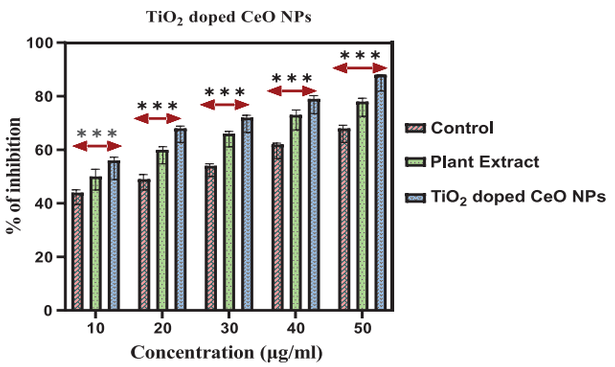

Figure 6. **Anti-diabetic potential of TiO_2 doped CeO Nanoparticles. Data from three replications are provided as mean ± SD. The data were statistically analysed using GraphPad Prism Software's one-way analysis of variance (ANOVA) and Dunnett's multiple range test (Tukey's post-hoc test). Statistically significant results are indicated by bars with the symbol "***" ($p < 0.005$).**

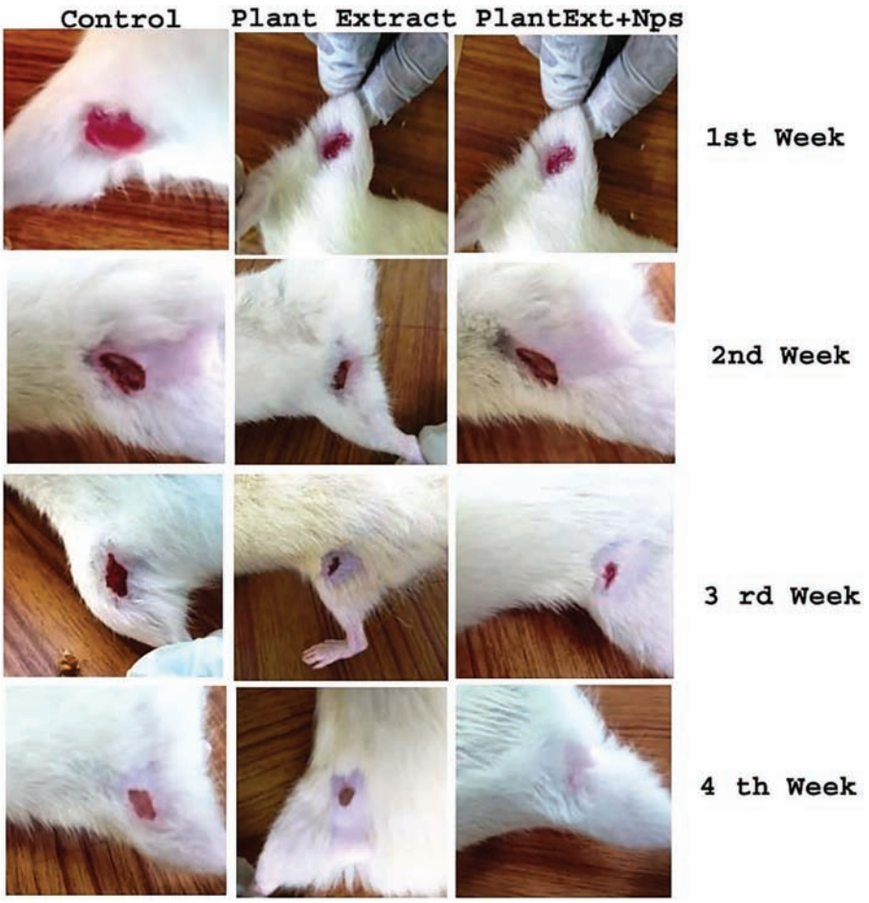

Figure 7. Macroscopic appearance of wound repair with Positive control, vehicle H_2O as control, *Rhinacanthus nasutus* Extract and TiO_2 doped CeO nanoparticles at different post wounding day.

the treatment was carried out for a duration of 10 consecutive days. Subsequently, we proceeded with a daily assessment of the morphological and behavioral alterations. All the animals in the study successfully completed the entire duration of the experiment without displaying any abnormalities [26]. The mice did not exhibit any toxicological concerns. For instance, one may observe symptoms such as fatigue, diminished appetite, alterations in fur pigmentation, and weight loss. The examination of hematologic parameters in control animals and animals subjected to TiO_2 doped CeO nanoparticles demonstrated only slight modifications in a small number of parameters. However, in general, there were no substantial variations observed [27]. The purpose of this study was to use histological observations made with a light microscope to learn more about the deleterious effects of nanoparticles on organ morphology.

The research conducted by Dr. MeenakshiSundaram from Tirunelveli Medical College Hospital in Tamil Nadu, India, has yielded results that confirm the absence of notable morphological alterations in the organs treated with TiO_2 doped CeO nanoparticles, as compared to the control organs. The histological examinations indicated that the liver, kidney, and lungs did not exhibit any toxic effects as a result of the presence of TiO_2 doped CeO nanoparticles, as shown in Figure 8.

The lung tissue histological sections obtained from the control animals displayed characteristic alveolar septa and proper alveolar structure (Fig. 8(A)). In a similar vein, the lung tissues that were subjected to treatment with titanium dioxide-doped cerium oxide nanoparticles displayed unaltered alveolar membranes and undamaged blood vessels, as depicted in Figure 8(B) [28]. The renal cortex and glomerular tufts in the kidney sections of control animals exhibited normal characteristics, as illustrated in Figure 8(C). Similarly, no discernible alterations were observed in the kidney tissue of animals subjected to gold nanoparticle treatment, as illustrated in Figure 8(D). The histological sections of the liver in the control animals displayed hepatic portals and central veins that exhibited normal characteristics (Fig. 8(E)). When comparing the liver samples, it was observed that the liver treated with titanium dioxide-doped cerium oxide nanoparticles

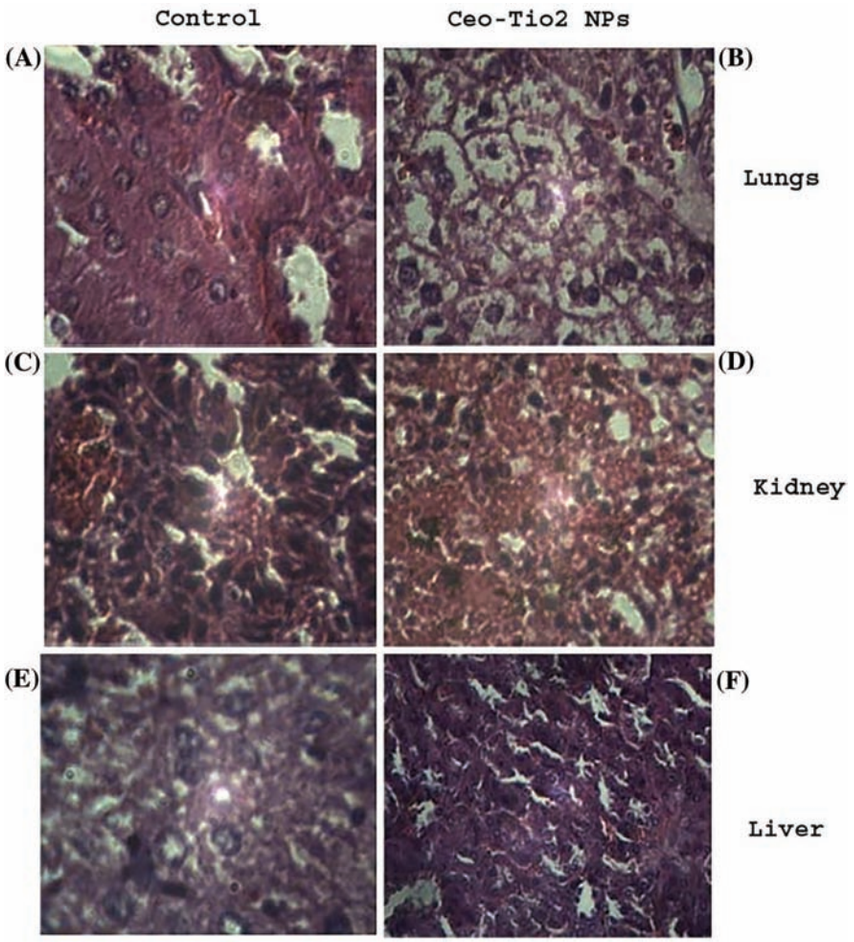

Figure 8. **Toxicity studies of TiO_2 doped CeO Nanoparticles in mouse organs.**

exhibited hepatocytes with normal morphology and a vein that appeared unaltered (Fig. 8(F)).

These experiments conclusively demonstrate that biologically produced TiO_2 doped CeO nanoparticles do not pose harm when utilized in an *in vivo* system. The histological investigations of vital organs such as the lung, kidney, and liver after a 10-day injection of TiO_2 doped CeO nanoparticles revealed no evidence of subclinical toxicity, further supporting the non-harmful impact of these particles.

Cytotoxicity

Biocompatibility of TiO_2 doped CeO Nanoparticle was demonstrated with brine shrimp lethality assay in Figure 9. In this study, doses of 10, 20, 30, 40, and 50 μg/ml of TiO_2 doped CeO Nanoparticle were studied to determine the survival rate of nauplii. For each concentration, a total of 10 live *Artemianauplii* were introduced. The Nauplii represent a developmental stage within the larval life cycle of copepods, offering convenient accessibility, affordability, and suitability for conducting short-term investigations [14]. On the first day of the experiment, all 10 nauplii in each concentration level were found to be alive. However, on the second day, a significant decline in nauplii count was observed alongside an increase in concentration, as depicted in Figure 9. This decline clearly indicated the cytotoxic effect of the solution [29]. Initially, all concentration levels had 10 live nauplii on the first day. However, at a concentration of 20 μL, there was a decrease in the count of nauplii from 10 to 9. When the concentration was reduced to 40 μL, the count decreased to 7. Likewise, when the concentration was adjusted to 60 μL, a mere 6 nauplii exhibited viability [30]. The number of viable nauplii remained constant at 6, even when the concentration was increased to 80 μL. Ultimately, when the concentration was adjusted to 50 μL, there was a complete absence of viable nauplii. The observed substantial disparity in nauplii count among various concentration levels provides clear evidence of cytotoxicity in the solution. Although CeO nanoparticles with a TiO_2 doping indicated toxicity, they can be employed to provide inhibitory effects [31]. It should be highlighted that the dose of TiO_2 doped CeO nanoparticles can be effective

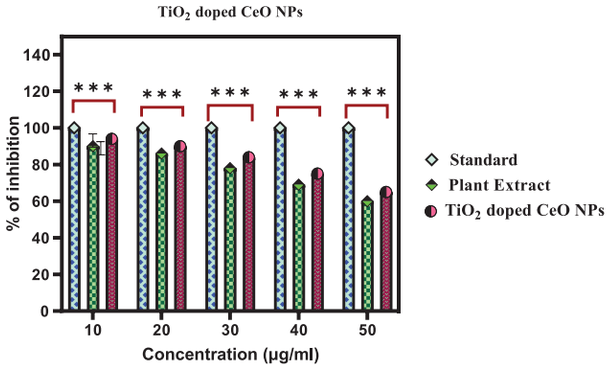

Figure 9. **The cytotoxicity image of TiO_2 doped CeO Nanoparticle using *R.nasutus* leaf extract. Data from three replications are provided as mean ± SD. The data were statistically analysed using GraphPad Prism Software's one-way analysis of variance (ANOVA) and Dunnett's multiple range test (Tukey's post-hoc test). Statistically significant results are indicated by bars with the symbol "∗∗∗" ($p < 0.005$).**

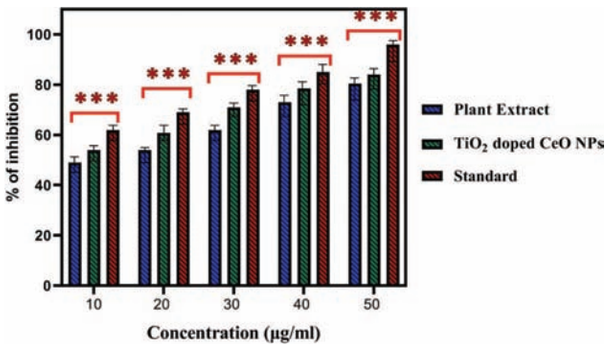

Figure 11. **Anti-inflammatory activity of TiO_2 doped CeO nanoparticles. Data from three replications are provided as mean ± SD. The data were statistically analysed using Graph Pad Prism Software's one-way analysis of variance (ANOVA) and Dunnett's multiple range test (Tukey's post-hoc test). Statistically significant results are indicated by bars with the symbol "∗∗∗" ($p < 0.005$).**

in cell viability based on the findings of the cell viability tests.

Antioxidant Activity of TiO_2 Doped CeO Nanoparticles

Figure 10 compares the *Rhinacanthus nasutus* plant extract to synthetic TiO_2 doped CeO nanoparticles and regular ascorbic acid in terms of free radical scavenging potential. At all concentrations used, *Rhinacanthus nasutus* aqueous extract demonstrated the highest % antioxidant potential [32]. It was discovered that this was dosage-independent, meaning that the scavenging ability was almost the same at 10 g/mL (the lowest dose) to 50 g/mL (maximum dose). TiO_2 doped CeO nanoparticles generated with aqueous

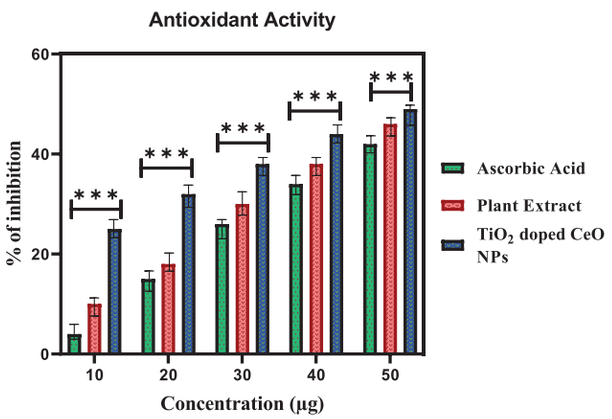

Figure 10. **Antioxidant Activity of TiO_2 doped CeO nanoparticles. Data from three replications are provided as mean ± SD. The data were statistically analysed using Graph Pad Prism Software's one-way analysis of variance (ANOVA) and Dunnett's multiple range test (Tukey's post-hoc test). Statistically significant results are indicated by bars with the symbol "∗∗∗" ($p < 0.005$).**

extract significantly decreased in scavenging ability, however this effect was dosage-dependent, ranging from 25% at 20 g/mL (minimum dose) to 49% at 50 g/mL. (Maximum dose). Similar to that, extract has a dose-dependent impact and is diminished when CeO nanoparticles are doped with TiO_2 [33]. The results of our study indicate a decrease in the antioxidant capacity of *Rhinacanthus nasutus* following its transformation into TiO_2-doped CeO nanoparticles. This observation suggests that the reducing photochemical may be utilized during the process of metal reduction.

Anti-Inflammatory Activity

In order to assess its anti-inflammatory properties, the reaction mixture was prepared in five different concentrations: 10 μL, 20 μL, 30 μL, 40 μL, and 50 μL. The effectiveness of the mixture was measured by determining the absorbance at various doses ranging from 10 to 50 μL. The absorbance percentages at these doses were found to be 54%, 60%, 71%, 78%, and 84%, respectively. Similarly, the absorbance percentages of the plant extract were determined to be 49%, 54%, 62%, 73%, and 80%, respectively. These results, depicted in Figure 11 [30], indicate the anti-inflammatory efficacy of the mixture.

Furthermore, a standard sample exhibited an 82% inhibition rate. Notably, when compared to regular diclofenac sodium, the highest anti-inflammatory activity was observed with *Rhinacanthus nasutus* extract mediated by TiO_2 doped CeO nanoparticles at a concentration of 50 μL [34].

CONCLUSION

The study focuses on the use of *Rhinacanthus nasutus* and artificially made TiO_2 doped CeO nanoparticles. The FT-IR spectra demonstrated the bio-capping of TiO_2

doped CeO nanoparticles, indicating the presence of bioactive functional groups that are commonly found in plant extracts. The characterisation of the TiO_2 doped CeO nanoparticles revealed their circular shape, rough surface morphology, and diameter of approximately 22 nm. The experiments conducted also showed that the created TiO_2 doped CeO nanoparticles had potent antioxidant and anti-inflammatory activities, effectively inhibiting the growth of DPPH radicals. These findings suggest that the synthetically produced TiO_2 doped CeO nanoparticles could have potential applications in various biomedical fields. Moreover, the method used in the study is simple, time-saving, and safe for the environment, as it does not involve the use of organic solvents, surfactants, or specialist equipment.

DECLARATIONS

Data Availability

The article incorporates all relevant data that substantiate the conclusions drawn in this study.

Competing Interests

The authors claim that the distribution of this manuscript does not involve any conflicts of interest.

Ethical Approval

The study received approval from the Administration Committee of Experimental Animals at M.S. University, located in Tirunelveli, Tamil Nadu.

Ethical Compliance

All human or animal research outlined in this paper has been approved by our institution's Ethical Committee and other appropriate authorities and has been conducted in conformity with all applicable standards, rules, legal constraints, and ethical standards.

Conflicts of Interest

There are no conflicts to declare.

Acknowledgment: Rajaduraipandian Subramanian (Register No: 20111232031009) acknowledges the research center Sri Paramakalyani College, Manonmaniam Sundaranar University, Alwarkurichi-627412, providing the support for this research work. This project was supported by Researchers Supporting Project number (RSP2023R230) King Saud University, Riyadh, Saudi Arabia.

REFERENCES

1. Joseph, T.M., KarMahapatra, D., Esmaeili, A., Piszczyk, Ł., Hasanin, M.S., Kattali, M., Haponiuk, J. and Thomas, S., **2023**. Nanoparticles: Taking a unique position in medicine. *Nanomaterials*, *13*, p.574. DOI: 10.3390/nano13030574.
2. Ibrahim, K., Khalid, S. and Idrees, K., **2019**. Nanoparticles: Properties, applications and toxicities. *Arabian Journal of Chemistry*, *12*, pp.908–931. DOI: 10.1016/j.arabjc.2017.05.011.
3. Farjadian, F., Ghasemi, A., Gohari, O., Roointan, A., Karimi, M. and Hamblin, M.R., **2019**. Nanopharmaceuticals and nanomedicines currently on the market: Challenges and opportunities. *Nanomedicine*, *14*, pp.93–126. DOI: 10.2217/nnm-2018-0120.
4. Lance, K., Eduardo, C., Lin, L.Z. and George, C.S., **2003**. The optical properties of metal nanoparticles: The influence of size, shape, and dielectric environment. *The Journal of Physical Chemistry B*, *107*, pp.668–677. DOI: 10.1021/jp026731y.
5. Prakash, J., Krishna, S.B.N., Kumar, P., Kumar, V., Ghosh, K.S., Swart, H.C., Bellucci, S. and Cho, J., **2022**. Recent advances on metal oxide based nano-photocatalysts as potential antibacterial and antiviral agents. *Catalysts*, *12*, p.1047. DOI: 10.3390/catal12091047.
6. Charbgoo, F., Ahmad, M.B. and Darroudi, M., **2017**. Cerium oxide nanoparticles: Green synthesis and biological applications. *International Journal of Nanomedicine*, *20*, pp.1401–1413. DOI: 10.2147/IJN.S124855.
7. Nadeem, M., Khan, R., Afridi, K., Nadhman, A., Ullah, S., Faisal, S., Mabood, Z.U., Hano, C. and Abbasi, B.H., **2020**. Green synthesis of cerium oxide nanoparticles (CeO_2 NPs) and their antimicrobial applications: A review. *International Journal of Nanomedicine*, *15*, pp.5951–5961. DOI: 10.2147/IJN.S255784.
8. So, J.P., Min, H., Ju, H.Y., Sung-Min, H., Choong, K.R., Jun-Gill, K. and Youngku, S., **2021**. Electrochemical Ce(III)/Ce(IV) redox behavior and Ce oxide nanostructure recovery over thio-terpyridine-functionalized Au/carbon paper electrodes. *ACS Appl. Mater. Interfaces*, *13*, pp.27594–27611.
9. Amutha, E., Sivakavinesan, M., Rajaduraipandian, S. and Annadurai, G., **2022**. Identification of phytochemicals capping the biosynthesized silver nanoparticles by wrightiatinctoria and evaluation of their in vitro antioxidant, antibacterial, antilarvicidal, and catalytic activities. *Emergent Materials*, *6*, pp.525–534. DOI: 10.1007/s42247-022-00422-7.
10. Varvoutis, G.L., Lykaki, M., Marnellos G.E. and Konsolakis, M., **2023**. Recent advances on fine-tuning engineering strategies of CeO_2-based nanostructure catalysts exemplified by CO_2 hydrogenation processes. *Catalysts*, *13*, p.275. DOI: 10.3390/catal13020275.
11. Weir, A., Westerhoff, P., Fabricius, L., Hristovski, K. and von Goetz, N., **2012**. Titanium dioxide nanoparticles in food and personal care product. *Environmental Science and Technology*, *46*, pp.2242–2250. DOI: 10.1021/es204168d.
12. Estévez, R., Eduardo, P., Joaquín, L.L. and Saravana, P.T., **2023**. Experimental studies on TiO_2 NT with metal dopants through Co-precipitation, sol–gel, hydrothermal scheme and corresponding computational molecular evaluations. *Materials*, *16*, p.3076. DOI: 10.3390/ma16083076.
13. Brimson, J.M., Prasanth, M.I., Malar, D.S., Brimson, S. and Tencomnao, T., **2020**. *Rhinacanthus nasutus* "Tea" infusions and the medicinal benefits of the constituent. *Phyto Chemicals Nutrients*, *12*, p.3776. DOI: 10.3390/nu12123776.
14. Puttarak, P., Charoonratana, T. and Panichayupakaranant, P., **2010**. Antimicrobial activity and stability of *Rhinacanthins*-rich *Rhinacanthus nasutus* extract. *Phytomedicine*, *17*, pp.323–327. DOI: 10.1016/j.phymed.2009.08.014.
15. Kartha, B., Thanikachalam, K., Natesan, V., Alharbi, N., Km, S. and Khaled, J., **2022**. Synthesis and characterization of Ce-doped TiO_2 nanoparticles and their enhanced anticancer activity in Y79 retinoblastoma cancer cells. *Green Processing and Synthesis*, *11*, pp.143–149.
16. Kavitha, K. and Sivakumar, A., **2022**. Synthesis and characterisation of cerium doped bismuth titanate proficient UV shielding and NIR reflective reddish brown pigment by citrate autocombustion synthesis. *Inorganic Chemistry Communications*, *136*, p.109162.

17. Khorrami, S., Zarrabi, A., Khaleghi, M., Danaei, M. and Mozafari, M., **2018**. Selective cytotoxicity of green synthesized silver nanoparticles against the MCF-7 tumor cell line and their enhanced antioxidant and antimicrobial properties. *International Journal of Nanomedicine*, *13*, pp.8013–8024.

18. Kumari M., Br E., Amberkar M., babu S., Rajshekar and Kumar N., **2010**. Wound healing activity of aqueous extract of crotalaria verrucosa in wistar albino rats asian pacific. *Journal of Tropical Medicine*, *3*, pp.783–787.

19. Latif, S., Tahir, K., Ullah Khan, A., Abdulaziz, F., Arooj, A., Alanazi, T.Y.A., et al., **2022**. Green synthesis of Mn-doped TiO_2 nanoparticles and investigating the influence of dopant concentration on the photocatalytic activity. *Inorganic Chemistry Communications*, *146*, p.110091.

20. Liu, Z., Guo, B., Hong, L. and Jiang, H., **2005**. Preparation and characterization of cerium oxide doped TiO_2 nanoparticles. *Journal of Physics and Chemistry of Solids*, *66*, pp.161–167.

21. Srinivasan, M., Venkatesan, M., Arumugam, V., Natesan, G., Saravanan, N., Murugesan, S., et al., **2019**. Green synthesis and characterization of titanium dioxide nanoparticles (TiO_2 NPs) using sesbaniagrandiflora and evaluation of toxicity in zebrafish embryos. *Process Biochemistry*, *80*, pp.197–202.

22. Cerrato, E., Gaggero, E., Calza, P. and Paganini, M.C., **2022**. The role of cerium, europium and erbium doped TiO_2 photocatalysts in water treatment: A mini-review. *Chemical Engineering Journal Advances*, *10*, p.100268.

23. Shanker, K., Mohan, G.K., Hussain, M.A., Jayarambabu, N. and Pravallika, P.L., **2017**. Green biosynthesis, characterization, in vitro antidiabetic activity, and investigational acute toxicity studies of some herbal-mediated silver nanoparticles on animal models. *Pharmacogn Mag.*, *13*, pp.188–192.

24. Miri, A., Sarani, M., Najafidoust, A., Mehrabani, M., Zadeh, F.A. and Varma, R.S., **2022**. Photocatalytic performance and cytotoxic activity of green-synthesized cobalt ferrite nanoparticles. *Materials Research Bulletin*, *149*, p.111706.

25. Nagar, H.K., Srivastava, A.K., Srivastava, R., Kurmi, M.L., Chandel, H.S. and Ranawat, M.S., **2016**. Pharmacological investigation of the wound healing activity of *Cestrum nocturnum* (L.) ointment in wistar albino rats. *Journal of Pharmaceutics*, *2016*, p.e9249040.

26. Naidi, S.N., Harunsani, M.H., Tan, A.L. and Khan, M.M., **2021**. Green-synthesized CeO_2 nanoparticles for photocatalytic, antimicrobial, antioxidant and cytotoxicity activities. *J. Mater. Chem. B*, *9*, pp.5599–5620.

27. Öztürk, İ., Beğiç, N., Bener, M. and Apak, R., **2021**. Antioxidant capacity measurement based on κ-carrageenan stabilized and capped silver nanoparticles using green nanotechnology. *Journal of Molecular Structure*, *1242*, p.130846.

28. Ponnanikajamideen, M., Devi Priya, S., Vanaja, M., Paulkumar, K., Rajeshkumar, S. and Annadurai, G., **2016**. In-vivo wound healing efficiency of curcumin loaded on chitosan polyvinyl propylene nanofilm. *Advanced Science, Engineering and Medicine*, *8*, pp.763–770.

29. Siriwatanametanon, N., Fiebich, B.L., Efferth, T., Prieto, J.M. and Heinrich, M., **2010**. Traditionally used Thai medicinal plants: In vitro anti-inflammatory, anticancer and antioxidant activities. *Journal of Ethnopharmacology*, *130*, pp.196–207.

30. Zubair, M., Azeem, M., Mumtaz, R., Younas, M., Adrees, M., Zubair E. et al., **2022**. Green synthesis and characterization of silver nanoparticles from *Acacia nilotica* and their anticancer, antidiabetic and antioxidant efficacy. *Environmental Pollution*, *304*, p.119249.

31. Ponnanikajamideen, M., Rajeshkumar, S., Vanaja, M. and Annadurai, G., **2019**. In vivo type 2 diabetes and wound-healing effects of antioxidant gold nanoparticles synthesized using the insulin plant *Chamaecostus cuspidatus* in albino rats. *Can. J. Diabetes*, *43*, pp.82–89.

32. Shakya, K., **2015**. Preparation of standardized *Rhinacanthus nasutus* leaf extract by green extraction methods and evaluation of antifungal activity of its topical solution against trichophytonrubrum. In 2015.

33. Zubair, M., Azeem, M., Mumtaz, R., Younas, M., Adrees, M., Zubair, E., et al., **2022**. Green synthesis and characterization of silver nanoparticles from Acacia nilotica and their anticancer, antidiabetic and antioxidant efficacy. *Environmental Pollution*, *304*, p.119249.

34. Subramanian, R., Eswaran, A., Kathirason, S.G., Ramar, S., Sivasubramanian, G., Alhadlaq, H.A., et al., **2022**. Green synthesized chitosan modified platinum-doped silver nanocomposite: An investigation for biomedical and environmental applications. *Journal of King Saud University-Science*, *34*, p.102220.